Acta Technica *62* (2017), No. 7A, 861–876

TSE robustness detection on semi-local damage flexibility of bridge structure health

Huang Li-pu[1], Feng Wan*[2,3], Hu Bai-qing[4], Chang Zhu-Gang[5], Huang Yang-zhou[1]

Abstract. In order to improve the robustness of bridge structure health detection algorithm to the time synchronization error (TSE) of synchronous protocol, a kind of semi-local TSE robustness test method of bridge structure health based on the damage flexibility method is proposed. This paper describes the semi-local TSE modal analysis and implementation method for frequency domain decomposition (FDD) of damage detection and positioning; Meanwhile, for the purpose of decreasing the data transmission from sensor node to the central unit, by virtue of semi-local processing method, this paper makes the local processing for every sensor node datum, makes the fast Fourier transform (FFT) for the detected vibration signal, transmits the obtained FFT value to the central unit or cluster head to make further processing, and then achieves the detection and localization of damage signals through flexibility method. The experimental result shows that, the method proposed by this paper is characterized by more sensitive damage detection performance, as well as stronger robustness of TSE influence.

Key words. Bridge structure effect, Structure health, Semi-local, Modal identification, Time synchronization error, Automatic monitoring

.

1. Introduction

In the structure health monitoring of the bridge, every kind of structure has a tendentious vibration, shown as the greater vibration amplitude on some frequencies

[1]School of civil engineering, Changsha University, Changsha, China
[2]School of electrical and information engineering, Hunan University, Changsha, China
[3]School of electronic information and electrical engineering, Changsha University, Changsha, China
[4]Guangdong China Communications Construction Consulting Co., Ltd, Foshan, China
[5]Guangdong China Communications Construction Consulting Co., Ltd, Foshan, China
*.corresponding author

than other frequencies [1∼2]. The theory of modal identification method is based on the influence of structure physical property on modelshape. For this reason, any physical property change of the structure may cause the detectable mode shape change. For the bridge detection, it mainly identifies and judges the external excitation source vibration incurred from wind load and traffic load, by a feat of the data fusion processing technology of wireless sensor network [3]. Aiming at the structure health detection of bridge, this paper carries out the algorithm design based on the method as shown in Literature [10]. However, different the centralized modal identification algorithm adopted in the Literature [10], this paper applies the semi-local modal identification method, and takes TSE problem of synchronous protocol into consideration at the same time, on the basis of damage flexibility, to achieve the bridge damage detection and localization based on WSNs detection signal.

2. System model and background

2.1. Background description

The system model adopted in this paper is similar to the model as shown in Literature [10], but, the difference is replacing the centralized processing with semi-local processing. Assuming that the wireless sensor network is equipped with n sensor nodes, the data is acquired with Sampling Frequency F_S and original data packet having Sample L. In the existing TSE index, the sensor acquisition data obtained at different times have the same sampling frequency. The schemes of centralized processing and semi-local processing are respectively as shown in Fig.1.

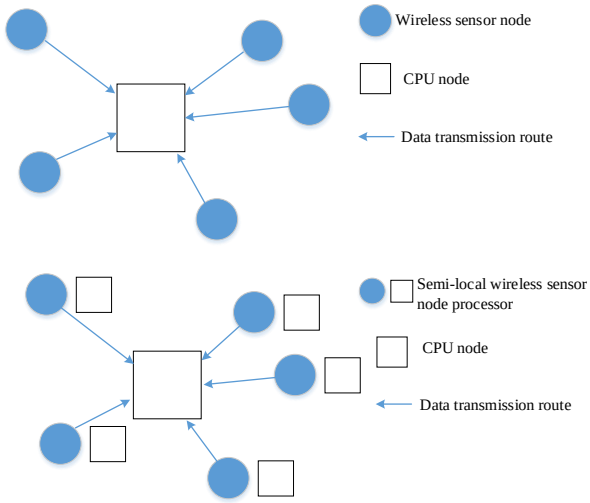

Fig. 1. Schemes of centralized processing & semi-local processing

In order to calculate the mode shape, the first FDD step is to determine the cross spectral density (CSD) of sensor output-signal matrix. Normally, the CSD matrix

can be determined by acquiring the mean CSD matrix through several data. The second CSD step is to apply the singular value decomposition (SVD) for the mean CSD matrix of every discrete frequency. The maximum values of singular value matrixes are collected into one vector, and the inherent frequency of the system can be identified from its peak value.

2.2. Data acquisition

The bridge structure health monitoring system designed in this paper contains three algorithm layers: (1) For data pre-processing; (2) Feature extraction layer; (3) Modal identification layer, the specific structure description of the system is as shown in Fig.2. For the purpose of verifying the efficiency of proposed system structure detection algorithm, the three-span bridges are selected to be the research objects. The wireless sensor nodes are set at the key joints of bridge structure, and the accelerated speed detected by the sensor will be transmitted at a specific sampling interval, specifically shown as:

$$D_i = \{d_1, d_2, \cdots, d_t, \cdots\} \ . \tag{1}$$

By operating the sampled sample data every day, the bridge structure status can be monitored.

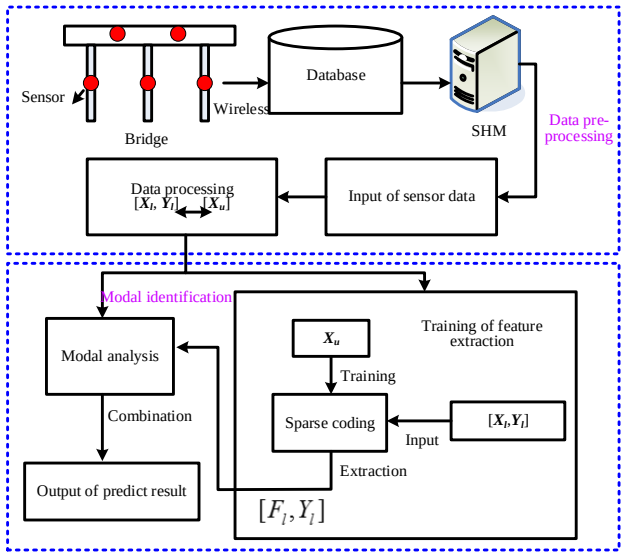

Fig. 2. Bridge structure monitoring system

In Fig.1, what in the Expression $[X_l, Y_l] \leftarrow [X_u]$ are the sample data and label, and $[F_l, Y_l]$ is the signal feature of bridge structure health.

2.3. Data pre-processing

The sensor sample data can be expressed as the time series or infinite vector. During the sample pre-processing process, segment the sample expressed by time series and express it to the form of time frame, as shown in Fig.3. In case the number of time frames attached to the bridge is r, the sampling frequency of Sensor R is f, and time frame is t. Connect the sample data in series and obtain:

$$x = (p_1, p_2, \cdots, p_r) \in R^{r \times t \times f}. \tag{2}$$

As the label is $y \in \{1, 2, \cdots, C\}$ and C is the number of modal types, the sample set $\{x, y\}$ can be built, and further obtain:

$$((x_l^{(1)}, y^{(1)}), (x_l^{(2)}, y^{(2)}), \cdots, (x_l^{(m)}, y^{(m)})\}. \tag{3}$$

$x_u^{(1)}, x_u^{(2)}, \cdots, x_u^{(k)} \in R^{r \times t \times f}$. If the bridge is in healthy status, the unlabeled form of k samples obtained is: $x_u^{(1)}, x_u^{(2)}, \cdots, x_u^{(k)} \in R^{r \times t \times f}$

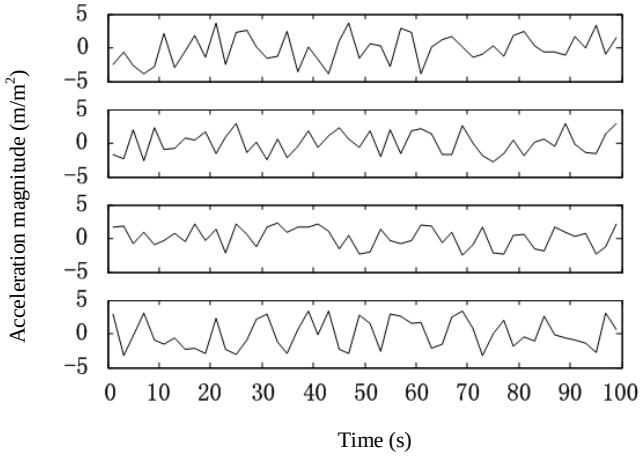

Fig. 3. Sample pre-processing

For the sparse coding process of feature, please refer to the relevant literatures, without unnecessary details given hereof.

3. Modal identification method

3.1. Centralized modal identification

According to the model as shown in Literature [10], considering the single sensor node in network as the reference sensor, all other sensor nodes try to make clock synchronization with the reference sensor. Assuming that two sensor nodes measure the acceleration data at the same location i, considering a sensor clock as reference

clock and its time as the reference time, the sensor acquires the data by reference clock, and other sensor nodes acquire the data their local clocks. At the same location i, the sampling data sets of reference node and other sensor nodes are respectively expressed as $x_i(t)$ and $\tilde{x}_i(t)$, and the relation of these two is shown as follows:

$$\tilde{x}_i(t) = x_i((1+\alpha_i)t + \delta t_i)\,. \tag{4}$$

Where, α_i is the clock drift rate, normally less than $50\mu s$; δt_i is the clock drift rate of other sensor nodes with respect to the reference sensor node. Therefore, for the relatively short frame, α_i can be ignored, and then obtain:

$$\tilde{x}_i(t) = x_i(t + \delta t_i)\,. \tag{5}$$

For the specific vibration mode structure, FFT transformation form of sensor node i to sample data $\tilde{x}_i(t)$ is:

$$\bar{X}_i(p) \approx X_i(p) e^{j\frac{2\pi\Delta n \cdot p}{N_f}}\,. \tag{6}$$

Where, $X_i(p)$ is the FFT transformation of sample $x_i(t)$; p is the discrete frequency index relevant to the inherent frequency of m order; N_f is the number of frequency samples outputted by FFT; Δn is the TSE expression of sample number. The TSE with given time is $\Delta n T_s = \Delta n / F_s$, where T_s is the sampling period. Set $w_m = 2\pi f_m$ is the angular frequency. Based on the phase deviation $w_m \delta t_i$, the FFT transformation form of $\tilde{x}_i(t)$ obtained is:

$$\bar{X}_i(p) \approx X_i(p) e^{j w_m \delta t_i}\,. \tag{7}$$

In order to identify the mode shape, the cross spectral density can be derived as:

$$\boldsymbol{D}(w_m) = \boldsymbol{D}(p) = \begin{bmatrix} X_1(p) \\ X_2(p) \\ \vdots \\ X_n(p) \end{bmatrix} \left[X_1^*(p), X_2^*(p), \cdots, X_n^*(p)\right] \tag{8}$$

For the SVD decomposition of CSD matrix made at location $w = w_m$ in the Formula (5), it can be calculated as:

$$\boldsymbol{D}(w_m)\boldsymbol{D}^*(w_m) = \boldsymbol{U} \sum \sum^* \boldsymbol{U}^* \tag{9}$$

In the formula, $\sum$ and $\boldsymbol{U}$ respectively are the singular value matrix and left singularity decomposition matrix. $\sum$ is the diagonal matrix containing feature value. The mth model shape assigned by $\boldsymbol{U}_1$ can be given at the first line of $\boldsymbol{U}$. CSD singular value decomposition relevant to incompletely synchronizing signals is given:

$$\tilde{\boldsymbol{D}}(\omega_m)\,\tilde{\boldsymbol{D}}^*(\omega_m) = \tilde{\boldsymbol{U}} \Sigma\Sigma\, \tilde{\boldsymbol{U}}^* \tag{10}$$

Similar to the complete synchronization, the first line of is $\tilde{\boldsymbol{U}}$ the model estimation

of order m, expressed as $\tilde{\boldsymbol{U}}_1$:

$$\tilde{U}_1 = \begin{bmatrix} e^{jw_m(\delta_{t_1}-\delta_{t_r})}\dfrac{U_{1,1}}{U_{r,1}} \\ e^{jw_m(\delta_{t_2}-\delta_{t_r})}\dfrac{U_{2,1}}{U_{r,2}} \\ \vdots \\ e^{jw_m(\delta_{t_n}-\delta_{t_r})}\dfrac{U_{n,1}}{U_{r,n}} \end{bmatrix} . \tag{11}$$

3.2. Semi-local modal identification

In the centralized processing sensor node i, for the original data acquisition, TSE index between the reference node and sensor node i can be calculated by utilizing δt_i. When a group of L samples are received by a sensor node, assume that it is suitable for making conducting calculation of original data received, and create N_f frequency sample which is sent to the intermediate node. Meanwhile, we think that, for every sensor node i, FFT frequency sample is transmitting based on TSE βt_i. For every sensor node i, FFT frequency sample $X_i(p)$, $i = 1, 2, \cdots, N_f$ is transmitting at a link experiencing TSE. The calculation form of is:

$$\beta t_i = \frac{\Delta p}{F_s} . \tag{12}$$

In the formula, Δp signifies the number of delay data samples received at central unit, and also signifies the number of delay samples $\tilde{X}_i(p)$ transmitted by FFT frequency sample. Assuming that we use the sample sampling frequency at the sending node and central node, and one received sample signifies a sample of FFT data packet sent by the sensor node, obtain:

$$\Delta p = \Delta n \frac{N_f}{F_s} . \tag{13}$$

Based on the centralized processing result of specific mode structure, the FFT transformation responding to $\tilde{x}_i(t)$ is similar to the structure as shown in Formula (4). For the specific node i, the number of delay samples in time domain are in direct proportion to the frequency. Hence, FFT frequency sample received by the central node can be signified as:

$$\tilde{Y}_i(p) = \tilde{X}_i(p + \Delta p) \approx \tilde{X}_i\left(p + \Delta n \frac{N_f}{F_S}\right) . \tag{14}$$

On account of different TSE among nodes, the Formula (14) can be signified as:

$$\tilde{Y}_i(p) = \tilde{X}_i(p + \beta p_i) . \tag{15}$$

Based on the Formula (7), with generalization made for n nodes, the Formula

(15) can be further expressed as:

$$\begin{bmatrix} \tilde{Y}_1(p) \\ \tilde{Y}_2(p) \\ \vdots \\ \tilde{Y}_n(p) \end{bmatrix} = \begin{bmatrix} X_1(p+\beta p_1)\, e^{jw_m(\delta t_1+\beta t_1)} \\ X_2(p+\beta p_2)\, e^{jw_m(\delta t_2+\beta t_2)} \\ \vdots \\ X_n(p+\beta p_n)\, e^{jw_m(\delta t_n+\beta t_n)} \end{bmatrix}. \tag{16}$$

Its vector form is:

$$\begin{aligned} \tilde{Y}(p) &= \begin{bmatrix} \tilde{Y}_1(p) \\ \tilde{Y}_2(p) \\ \vdots \\ \tilde{Y}_n(p) \end{bmatrix}^T = \begin{bmatrix} X_1(p) \\ X_2(p) \\ \vdots \\ X_n(p) \end{bmatrix}^T * \begin{bmatrix} \delta(p+\beta p_1) \\ \delta(p+\beta p_2) \\ \vdots \\ \delta(p+\beta p_n) \end{bmatrix} \begin{bmatrix} e^{jw_m(\delta t_1+\beta t_1)} \\ e^{jw_m(\delta t_2+\beta t_2)} \\ \vdots \\ e^{jw_m(\delta t_n+\beta t_n)} \end{bmatrix}^T \\ &= (X(p) * \Delta) P \end{aligned} \tag{17}$$

Where, $\boldsymbol{X}(p)$ is the input test vector given in the frequency domain; the symbol "*" signifies the consideration of convolution operation of frequency p; Δ is the Dirac pulse vector displacement in frequency domain. In the frequency domain, TSE given by βp_i can be regarded as the frequency displacement of βp_i and then taken as the convolution of receipt signal, of which its Dirac δ function is $\delta(p+\beta p_i)$. This δ function creates a displacement corresponding to $\tilde{X}_i(p)$ and $\tilde{Y}_i(p)$. In order to achieve the model identification of $\tilde{\boldsymbol{Y}}(p)$, the cross-spectral density function form is:

$$\begin{aligned} \tilde{\boldsymbol{D}}_y(w_m) = \tilde{\boldsymbol{D}}_y(p) &= \begin{pmatrix} \tilde{Y}_1(p) \\ \tilde{Y}_2(p) \\ \vdots \\ \tilde{Y}_n(p) \end{pmatrix} \begin{pmatrix} \tilde{Y}_1^*(p) & \tilde{Y}_2^*(p) & \cdots & \tilde{Y}_n^*(p) \end{pmatrix} \\ &= \boldsymbol{P}^T \left(\boldsymbol{X}^T(p) * \Delta^T \right) \left(\boldsymbol{X}^*(p) * \Delta^* \right) \boldsymbol{P}^*. \end{aligned} \tag{18}$$

In order to achieve the modal identification, for the perfect synchronization, make eigenvalue decomposition on $\tilde{\boldsymbol{D}}_y(w_m)$ and $\tilde{\boldsymbol{D}}_y^*(w_m)$, the delay due to Δ in the vector $\boldsymbol{X}(p)$ can be known, with following form obtained:

$$\left(\boldsymbol{X}^T(p) * \Delta^T \right) \left(X^*(p) * \Delta^* \right) = \begin{bmatrix} A_0 & B_0^T \\ B_0 & C_0 \end{bmatrix}. \tag{19}$$

According to the Formula (15), the prdocut of $\tilde{\boldsymbol{D}}_y(w_m)$ and $\tilde{\boldsymbol{D}}_y^*(w_m)$ can be decomposed as follows:

$$\tilde{\boldsymbol{D}}_y(w_m)\, \tilde{\boldsymbol{D}}_y^*(w_m) = \begin{bmatrix} A & B^T \\ B & C \end{bmatrix}. \tag{20}$$

Based on above two forms, by virtue of the relation among A_0, B_0 and C_0, as well as A, B and C, the eigenvalue decomposition form of $\tilde{\boldsymbol{D}}_y(w_m)\, \tilde{\boldsymbol{D}}_y^*(w_m)$ can be

deduced.

4. Damage detection and location based on time synchronization

4.1. Damage flexibility method

Flexibility method is a kind of damage detection method based on vibration, for determining the damage happened in the structure. By using the flexibility method, the damage identification is made through the change of data frequency response. The flexibility $\boldsymbol{F}$ can be determined by using several kinds of basic modes of following basic modal parameters [11∼13].

$$F = \sum_{m=1}^{N} \frac{1}{(w_m)^2} \phi_m \phi_m^T N \,. \tag{21}$$

Where, ϕ_m is the normalized mode of m order concerning the modal frequency w_m, and N is the number of low-frequency modes applied in the deduction process.

4.2. (DLV)Damage locating vector

The damage locating vector can be defined as the null space basis of flexibility change, so that, the calculation can be made not by reference to the modal structure, but according to the measured data. The stress field for locating the damage can be calculated by virtue of specific structure mode, but meanwhile, the damage location with DLV technology also cannot avoid the existence of model error. The advantage of DLV method needn't to measure all freedom structure responses, although few sensors may give rise to limited damage detection capacity. However, this method is of certain insensitivity for the error source, for the reason that only the topological structure and relative stiffness parameter are used for stress calculation. Normally, DLV technology can be applied on the basis of mode truncation and be of the ability to process single or multiple damage scenarios for sensor nodes at any quantity.

Firstly, the flexibility matrixes at the sensor position can be built according to the measurement data before and after damage, which can respectively expressed as $\boldsymbol{F}_U$ and $\boldsymbol{F}_D$. Then, through the derivation of flexibility difference, the variation form of flexibility can be obtained as follows [14∼15]:

$$\boldsymbol{F}_\Delta = \boldsymbol{F}_U - \boldsymbol{F}_D \,. \tag{22}$$

Bernhardt develops a kind of common damage location method for extracting the flexibility variation of spatial information. The damage locating vector DLVs can be obtained SVD decomposition of $\boldsymbol{F}_\Delta$, with form as:

$$\boldsymbol{F}_\Delta = \boldsymbol{U}\boldsymbol{S}\boldsymbol{V}^T = [\boldsymbol{U}_1, \boldsymbol{U}_0] \begin{bmatrix} \boldsymbol{s}_1 & \boldsymbol{0} \\ \boldsymbol{0} & \boldsymbol{0} \end{bmatrix} \begin{bmatrix} \boldsymbol{V}_1^T \\ \boldsymbol{V}_0 \end{bmatrix} . \tag{23}$$

A vector can be extracted from the diagonal element or every line of maximum absolute value in $\boldsymbol{F}_{\Delta}$, and the damage location can be made on this basis, by virtue of SVD characteristics:

$$\begin{bmatrix} \boldsymbol{V}_1^T \\ \boldsymbol{V}_0 \end{bmatrix} [\boldsymbol{V}_1 \quad \boldsymbol{V}_0] = \boldsymbol{I} \,. \tag{24}$$

Where, $\boldsymbol{I}$ is the unit matrix. The Formula (19) can be rewritten as:

$$[\boldsymbol{F}_{\Delta}\boldsymbol{V}_1 \quad \boldsymbol{F}_{\Delta}\boldsymbol{V}_0] = [\boldsymbol{U}_1\boldsymbol{S}_1 \quad 0] \,. \tag{25}$$

According to the above formula, obtain:

$$\boldsymbol{F}_{\Delta}\boldsymbol{V}_0 = 0 \,. \tag{26}$$

In order to make DLV selection in $\boldsymbol{V}$, define:

$$svn_i = \sqrt{\frac{s_i c_i^2}{s_q c_q^2}} \,. \tag{27}$$

Where, $s_q c_q^2 = \max\left(s_i c_i^2\right)$ and $i = 1, 2, \cdots, m$; by virtue of the maximum value of $s_i c_i^2$ given by q of index i, m is the quantity of lines in $\boldsymbol{V}$; s_i is the ith singular value of matrix $\boldsymbol{F}_{\Delta}$; c_i is the constant to normalize the maximum characteristic stress of undamaged structural elements, which is correlate to the static load $c_i\boldsymbol{V}_i$, equal to 1. If $svn_i \leq 0.20$, the vector $\boldsymbol{V}_i$ can be taken as DLV. Then, make damage location for the unknown damage structure by virtue of DLV, and calculate the characteristic stress of every structure unit. For every DLV vector, the normalized stress $\bar{\sigma}_i$ in element i can be defined as:

$$\bar{\sigma}_i = \sigma_i / \sigma_q \,. \tag{28}$$

Where, σ_i is the element stress given by every cross-section stress, $\sigma_q = \max(\sigma_i)$ and $i = 1, 2, \cdots, m$. q is the index i corresponding to the maximum value of σ_i. In order to strengthen the algorithm robustness, multi-DLVs information fusion method can be adopted:

$$WSI = \frac{\sum_{i=1}^{ndlv} \bar{\sigma}_i / E\left(svn_i\right)}{ndlv} \tag{29}$$

Where, $ndlv$ is the number of DLVs, and the elements with damage determined are $WSI < 1$ and $E\left(svn_i\right) = \max\left(svn, 0.015\right)$. See Algorithm 1 for the damage detection and location steps.

Algorithm 1: Damage detection and location

1. **procedure** MODE SHAPE IDENTIFICATION $x_i(t)$, δt_i, βt_i
2. $\%x_i$ measured acceleration value; TSE of δt_i local node; TSE of βt_i centralized node
3. $X_i(p) \leftarrow FFT(x_i(t))$;
4. $\tilde{X}_i(p) \leftarrow FFT(x_i(t+\delta t_i))$;
5. $\tilde{Y}_i(p) \leftarrow \tilde{X}_i(p+\beta p_i)$;
6. $\boldsymbol{D}(w_m) \leftarrow csd(X_1, X_2, \cdots, X_n)$;
7. $SVD(\boldsymbol{D}(w_m)\boldsymbol{D}(w_m)^*) = \boldsymbol{U}\sum\sum^*\boldsymbol{U}^*$;
8. return ϕ_i
9. **procedure** DAMAGE LOCALIZATION ϕ_i, w_i
10. $F \leftarrow \sum_{i=1}^{N} \frac{1}{(w_i)^2}\phi_i\phi_i^T$;
11. $(DLV)\, F_\Delta \leftarrow F_U - F_D$;
12. $SVD(F_\Delta) \leftarrow U\sum\sum^* U^*$;
13. $svn_i = \sqrt{\frac{s_i c_i^2}{\max_k(s_k c_k^2)}}$, $i = 1, 2, \cdots, m$;
14. $WSI = \frac{\sum_{i=1}^{ndlv} \bar{\sigma}_i / E(svn_i)}{ndlv}$;
15. ***if*** $(WSI < 1)$ ***then***
16. ***return*** Structure damaged
17. ***else***
18. ***return*** Structure undamaged

5. Experimental analysis

5.1. Experiment setting

The three-span bridge is considered, which is built by virtue of Matlab structural dynamics tool kit, consisting of 150 nodes and 182 elements. The bridge surface is set to be 80m long and 8m wide, including two traffic lanes. The bridge is made of steel, with Young modulus and shear elasticity modulus respectively set to be 210GPa and 80GPA. The properties of main materials used in the experiment are listed in the Table 1. However, if the bridge is damaged or corroded, these two parameters will decrease following the damage or corrosion degrees. This system is stimulated by the even pressure acting on the whole bridge surface, and the bridge motion is only restricted to the plane vibration. The left and right edges as well as three pier bases of bridge surface are fixed.

Table 1. Material characteristics of steel

Sympbol	Value	Unit	Physical description
Nu	0.285		Poisson's ratio
E	210000000000	Pa	Young's
G	81712062256	Pa	Shear
Rho	7800	Kg/m3	Density
Alpha	0	/oC	Thermal
Eta	0	Loss	factor
T0	20	oC	Reference

In order to monitor the bridge status, set 36 tri-axis accelerometers on the upper and bottom surfaces of bridge, as well as the juncture between the bridge surface and pier. Sensor sampling frequency is set at 5Hz. Every sensor records 5 groups of acceleration data per 1s. Hence, during the monitoring period, the data recorded by one sensor can be deemed as the one-dimensional vector, while the data collected by 36 groups of sensors can constitute the matrix. These sensor data are original data and can be used after feature extraction.

The bridge condition in the real world may easily be influenced by the environment factors, such as wind, temperature, humidity and even the slight disturbance, which may cause the change of acceleration data collected by the sensor. For the purpose of enabling the experiment to be real to the greatest extent, all environmental noise obeys the Gaussian distribution with zero mean and standard deviation. The reason is that, all environmental factors cannot be listed out and the leading role of factor cannot be determined, so that the safest method is assuming all factors obey the Gaussian distribution. Based on above assumptions, aiming at every sample datum, the environmental noise is added by:

$$\alpha_i(t) = \alpha_i(t) + N(0,\sigma)(t) \ . \tag{30}$$

Where, $\alpha_i(t)$ is the acceleration data measured by the sensor i at the time t. $N(0,\sigma)$ is the Gaussian random variable with mean value 0 and variance σ. $\sigma = 1$ and $\sigma = 0.5$ are respectively considered in the experiment.

Make original data sampling at every sensor node. TSE δt_i is considered to be a random variable within following sections: $[0, 10/F_s]$, $[0, 20/F_s]$ and $[0, 30/F_s]$, which also an measure the FFT frequency sampling during the transmission period. In this experiment, set $n = 25$ sensor nodes in the wireless sensor network. What TSE concerns are front 14 data samples of original sampling data – δt_i =[5, 1, 14, 14, 19, 8, 11, 17, 1, 2, 11, 14, 1, 8]t_i, as well as the FFT frequency samples transmitted to the central unit –βt_i =[0; 2; 1; 4; 0; 0; 0; 0; 0; 0; 0; 0; 0; 0]t_i.

In this paper, simulate the time series and response by using 10,000 acceleration points which are generated by virtue of famous integral method. For the semi-local processing process, TSE, incurred during the transmission process of FFT frequency sampling from the sensor node to the central unit, can be deemed as random variable: $[0, 10/F_s]$, $[0, 20/F_s]$ and $[0, 30/F_s]$. Next, analyze the simulated time series and response by applying the semi-local and centralized processing FDD method.

During the experiment process, the evaluation on influence of TSE on modal identification and damage detection is considered. During the process of original data acquisition of every sensor node, TSE is δt_i. During the original data acquisition process, TSE δt_i can be deemed as the uniform random variable within the section $[0, 20/F_s]$. The simulated TSE relevant to the FFT frequency sampling transmitted to the central unit is $[\beta p_1; \beta p_2; \cdots; \beta p_{25}] = [0; 2; 1; 4; \mathbf{0}_{21}]/F_s$, of which $\mathbf{0}_{21}$ is 21D 0-element vector. The power spectrum density of semi-local processing center unit signal is given in the Fig.4.

In the figure, limited by the space, only four sensor nodes are tested hereof. The FFT frequency sampling transmitted from the sensor node to the central node has similar frequency deviation.

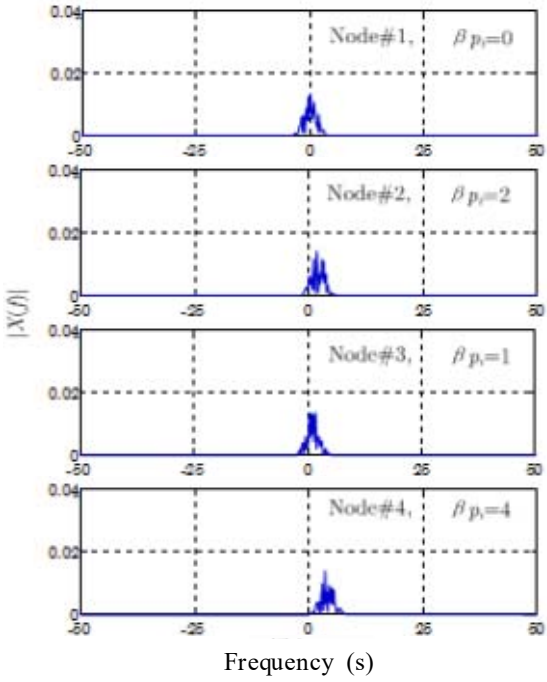

Fig. 4. Power spectrum density of incompletely synchronous response of local processing

5.2. Damage location and time synchronization error

Because TSE error can give rise to the distortion of identified mode shape, the determination of power spectrum density of output response as shown by the algorithm in Literature [15] is the improved FFT method based on incomplete synchronization samples, which is a kind of typical centralized method. The parameter settings of two algorithms: , an . The comparison results of deficiency damage detection probability and destruction detection probability of the algorithms in this paper and the

Literature [15] are as shown in Fig.5.

From the result in Fig.5, it can be known that, compared with the algorithm of Literature [15], both of the deficiency damage detection probability and destruction detection probability have smaller probability values, showing higher detection accuracy of algorithm in this paper. Meanwhile, it can be seen that, in cases of and, the deficiency damage detection probability index of the algorithm in this paper is different from that of its destruction detection probability index. It can be seen that, $\beta p_i = 30/F_s$ is of higher deficiency damage detection probability and destruction detection probability than $\beta p_i = 10/F_s$, as well as poorer detection effect.

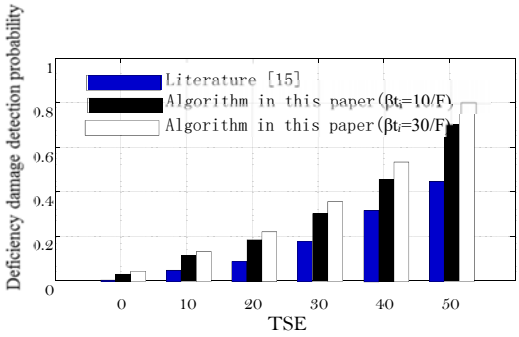

(a) Deficiency damage detection probability

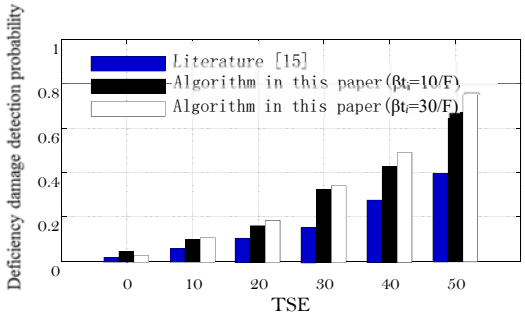

(b) Destruction detection probability

Fig. 5. Damage detection probability

5.3. Performance influence of FFT output length

The first step of modal analysis is from the FFT calculation of measured original data. In this part, we research the FFT frequency resolution method of modal analysis and carry out the similarity test of complete and incomplete synchronization. Assume the transmission of a group of original data packages with length of $L = 2048$ and sampling frequency of $F_s = 200Hz$. Define F_s/N_f as $\left\{\frac{F_s}{256}, \frac{F_s}{512}, \frac{F_s}{1024}\right\}$, adjust the FFT frequency resolution. According to the time migration derivative and its

influence on frequency error in the semi-local modal identification, it can be proved that, if considering the time migration of Δn samples, FFT value will be translated for Δn samples, of which $\Delta p = \Delta n N_f / F_s$. The comparison of deficiency damage detection probability and destruction detection probability in different valuation cases is as shown in Fig.6.

In Fig.6, in the semi-local modal identification algorithm, the influence of FFT output length on deficiency damage detection probability (see Fig.4a) and destruction detection probability (see Fig.4b) is given, of which TSE can be defined as: $\delta t_i = 10/F_s$ and $\beta p_i \in \{10/F_s, 30/F_s\}$. Two main conclusions can be obtained: (1) When using low-resolution FFT algorithm, the damage cannot be detected out, mainly for the performance degradation of modal identification algorithm caused by lower N_f valuation; (2) The higher the TSE value is taken, the higher the false dismissal probability is caused. Where $N_f = 1024$ can be accepted, for the reason that the detection probability in such valuation does not decrease sharply, and the balance between the data size and detection accuracy can be realized.

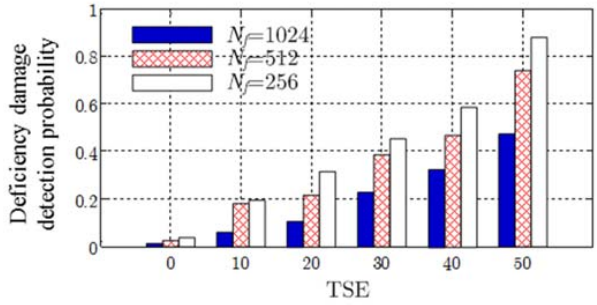

(a) Deficiency damage detection probability

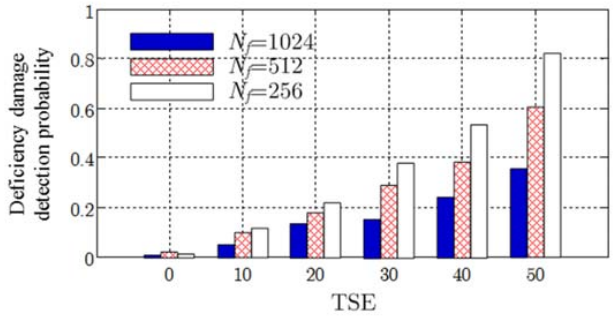

(b) Destruction detection probability

Fig. 6. Performance impact of FFT output length

6. Conclusions

Aiming at the bridge structure health, by equipping with wireless sensor network, the semi-local TSE robustness detection method of bridge structure health based on

damage flexibility method is built. In order to reduce the data transmission from the sensor node to the central unit, by virtue of semi-local processing method, make local processing for the data of every sensor node, conduct the fast Fourier transform for the detected vibration signals, transmit the acquired FFT value to the central unit or cluster head for further processing, and achieve the damage signal detection and location through the flexibility method, to obtain the better damage detection effect.

Acknowledgement

Scientific Research Project of Changsha Science and Technology Bureau–Internet Plus in the Development of Structural Health Monitoring System for Existing Bridge (ZD1601023); Scientific Research Project of Hunan Province Education Department-Study of Load Transverse Distribution Coefficient in Widening and Strengthening of Old Bridge (15C0125).

References

[1] M. P. Malarkodi, N. Arunkumar, V. Venkataraman: *Gabor wavelet based approach for face recognition*, International Journal of Applied Engineering Research, *8* (2013), No. 15, 1831–1840.

[2] L. R. Stephygraph, N. Arunkumar: *Brain-actuated wireless mobile robot control through an adaptive human-machine interface*, Advances in Intelligent Systems and Computing, *397* (2016), 537–549.

[3] N. Arunkumar, V. Venkataraman, T. Lavany : *A moving window approximate entropy based neural network for detecting the onset of epileptic seizures*,International Journal of Applied Engineering Research, *8* (2013), No. 15, 1841–1847.

[4] J. W. Chan, Y. Y. Zhang, and K. E. Uhrich: *Amphiphilic Macromolecule Self-Assembled Monolayers Suppress Smooth Muscle Cell Proliferation*, Bioconjugate Chemistry, *26* (2015), No. 7, 1359–1369.

[5] Y. J. Zhao, L. Wang, H. J. Wang, and C. J. Liu: *Minimum Rate Sampling and Spectrum Blind Reconstruction in Random Equivalent Sampling.* Circuits Systems and Signal Processing, *34* (2015), No. 8, 2667–2680.

[6] S. L. Fernandes, V. P. Gurupur, N. R. Sunder, N. Arunkumar, S. Kadry: *A novel nonintrusive decision support approach for heart rate measurement*, (2017) Pattern Recognition Letters. https://doi.org/10.1016/j.patrec.2017.07.002

[7] N. Arunkumar, K. Ramkumar, V. Venkatraman, E. Abdulhay, S. L. Fernandes, K S. adry, & S. Segal: *Classification of focal and non focal EEG using entropies.* Pattern Recognition Letters, *94* (2017), 112–117.

[8] W. S. Pan, S. Z. Chen, Z. Y. Feng.: *Investigating the Collaborative Intention and Semantic Structure among Co-occurring Tags using Graph Theory.* International Enterprise Distributed Object Computing Conference, IEEE, Beijing, (2012), 190–195.

[9] Y. Y. Zhang, Q. Li, W. J. Welsh, P. V. Moghe, and K. E. Uhrich: *Micellar and Structural Stability of Nanoscale Amphiphilic Polymers: Implications for Anti-atherosclerotic Bioactivity*, Biomaterials, *84* (2016), 230–240.

[10] L. R. Stephygraph, N. Arunkumar, V. Venkatraman: *Wireless mobile robot control through human machine interface using brain signals*, 2015 International Conference on Smart Technologies and Management for Computing, Communication, Con-

trols, Energy and Materials, ICSTM 2015 - Proceedings, (2015), art. No. 7225484, 596–603.

[11] N. Arunkumar, V. S. Balaji, S. Ramesh, S. Natarajan, V. R. Likhita, S. Sundari: *Automatic detection of epileptic seizures using independent component analysis algorithm*, IEEE-International Conference on Advances in Engineering, Science and Management, ICAESM-2012, (2012), art. No. 6215903, 542–544.

[12] Y. Du, Y. Z. Chen, Y. Y. Zhuang, C. Zhu, F. J. Tang, J. Huang: *Probing Nanostrain via a Mechanically Designed Optical Fiber Interferometer.* IEEE Photonics Technology Letters, *29*(2017), 1348–1351.

[13] W. S. Pan, S. Z. Chen, Z. Y. Feng:*Automatic Clustering of Social Tag using Community Detection.* Applied Mathematics & Information Sciences, *7* (2013), No. 2, 675–681.

[14] Y. Y. Zhang, E. Mintzer, and K. E. Uhrich: *Synthesis and Characterization of PEGylated Bolaamphiphiles with Enhanced Retention in Liposomes*, Journal of Colloid and Interface Science, *482* (2016), 19–26.

Received May 7, 2017